Spring-magnet oscillations through a bored conductive plate

Celso L. Ladera, **Guillermo Donoso and Pablo Martín**
Departamento de Física, Universidad Simón Bolívar, Apdo. 89000, Caracas 1086, Venezuela.

E-mail: clladera@usb.ve

(Received 5 January 2014, accepted 16 March 2014)

Abstract

Low frequency vertical oscillations of a spring-magnet system through an orifice bored in a non-magnetic metallic plate are here introduced and studied. In spite of the clean crossings of the magnet through the orifice a magnetic force between plate and magnet still dampens oscillations of this system. We build a theoretical model of the spring-magnet motion that leads us to its motion equation. This happens to be a third degree second-order differential that we solve for the case in which the magnet executes small amplitude oscillations. The model allowed us to predict the functional dependences of the magnet motion variables that we then confirmed experimentally in the laboratory. It is a low-cost oscillating system useful for both its physics content and its mathematical modelling, one that can be easily set-up and studied with parts and equipment ordinarily found in a physics laboratory. This work is within the reach of undergraduate students of physics and engineering students, and can be exploited either as an experiment in an intermediate physics laboratory or as an open-end project work.

Keywords: Damped nonlinear oscillations, Magnetic induction, Magnetic damping, Physics teaching experiments.

Resumen

Presentamos y estudiamos las oscilaciones verticales de un sistema formado por un imán que cuelga de un resorte, y que oscila a través de un orificio horadado en una placa metálica no-magnética. El magneto pasa a través del orificio sin tocar sus bordes, pero aún así se genera una fuerza magnética que amortigua las oscilaciones del sistema. Hemos construido un modelo teórico de estas oscilaciones que nos condujo a su ecuación de movimiento. Ésta resulta ser una ecuación diferencial no lineal de segundo orden la cual resolvemos aquí para el caso en el cual el sistema oscila con pequeña amplitud. El modelo nos ha permitido predecir las dependencias funcionales del movimiento del imán que luego hemos confirmado experimentalmente en el laboratorio. Se trata de un sistema oscilante de bajo costo que ha de resultar muy útil debido a la física-matemática utilizada para modelarlo. Es sin duda un oscilador que puede ser fácilmente construido y estudiado con componentes y equipos de uso corriente en laboratorios de física. El trabajo está al alcance de estudiantes de pregrado en física o ingeniería, y puede ser explotado bien como experimento de un laboratorio intermedio de física, o bien como un proyecto que tenga fines abiertos.

Palabras clave: Oscilaciones amortiguadas no lineales, inducción magnética, amortiguación magnética, experimentos de enseñanza de Física.

PACS: 75.80.+q, 41.20.Gz, 01.50.Pa, 72.15.Cz, 01.50.My **ISSN 1870-9095**

I. INTRODUCTION

Several magneto-mechanical oscillators have been recently presented in the literature [1, 2, 3, 4, 5, 6]. Fig. 1 depicts an entirely new one: a magnet that oscillates vertically, and with low frequency through an orifice of radius *a* bored in a non ferromagnetic metallic plate. The case of a magnet that oscillates above a whole plate [6] was recently studied, and the present case was therefore natural to consider. It leads to a very different analytical treatment, and to entirely different results. These oscillations are damped by the weak magnetic interaction force between the bored plate and the moving magnet, *i.e*. by the interaction force between magnet and conductor as observed in other cases of magnet motion [4, 5, 6, 7, 8, 9], but this time the theoretical model of the magnet motion leads to a highly non-linear second order differential equation that can be solved in a number of ways. For the sake of a simplified mathematical and pedagogical treatment here we solve the system motion equation in Section II by assuming the oscillations of the magnet to be small and weakly damped by the magnetic force, and by equating the total energy change in the *n-th* cycle of oscillation to the energy lost by damping in the same cycle. This is in fact a very useful procedure

described by Landau and Lifshitz in the mechanics book of their well-known theoretical physics course [10]. For the present oscillating system the procedure leads to a quadratic algebraic equation that relates the initial amplitude A_n of oscillation in the *n*-th cycle to the amplitude of oscillation A_0 at the start of the oscillations. The oscillator shown in Fig. 1 can be easily set-up in the laboratory using a small neodymium magnet, and bored aluminium plates of different thicknesses. In Section II we develop our analytical model of the magnet motion, and find its nonlinear motion equation. After giving the actual details of our spring-magnet oscillator in Section III and of our experimental set-up, we present our experiments and results in Section IV, and compare the latter with the predictions of our analytical model. Finally we discuss the work and present our conclusions in Section V.

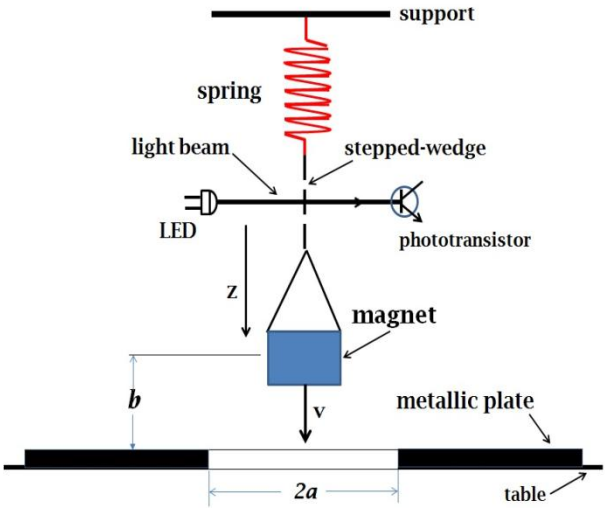

FIGURE 1. A magnet hangs from a spring and oscillates along the vertical *z*-axis through an orifice of radius *a* in a conducting non-magnetic plate. The equilibrium distance from magnet to plate is *b*<<*a*. A transparent stepped-wedge modulates a collimated light beam from a LED and transduces the magnet position into an electrical signal (after detection with a phototransistor).

II. ANALITYCAL MODEL OF THE MAGNET MOTION

The dominant forces acting on the oscillating magnet in Fig. 1 are of course: its own weight, the elastic force applied by the spring as the magnet oscillates, and finally the magnetic dragging force applied to the magnet by the weak Foucault (eddy) currents induced in the plate by the moving magnet itself. The friction of the whole oscillating system with the surrounding air was previously measured and found to be negligible in comparison. The magnetic dragging force has been calculated in many works, and in a number of altogether different instances [3, 4, 5, 6, 7, 8, 9, 12]. We need to recalculate it here in the light of the present set-up: thus consider an infinitesimal ring of the conducting plate, of radius $r>a$ and width dr, coaxial with the main axis of symmetry of the magnet, and with the orifice, as shown in Fig. 2. The equilibrium vertical position of the magnet is represented by *b*.

Since the magnet approaches the orifice with speed *v* a motional *e.m.f.* ε_i is induced in the conducting infinitesimal ring element. This *e.m.f.* can be obtained by applying Faraday´s Law ($\varepsilon_i = \int(\boldsymbol{v}\times\boldsymbol{B}).d\boldsymbol{l}$) [6, 12, 13]:

$$\varepsilon_i = 2\pi r B_\rho(r,b)v, \qquad (1)$$

where B_ρ denotes the radial component of the magnet field. If τ denotes the thickness of the plate, and σ its electrical conductivity, the electrical current *di* that appears in the infinitesimal ring is given by the induced *e.m.f.* ε_i times the conductance $G = (\sigma\tau dr)/2\pi r$ of the ring *i.e.*

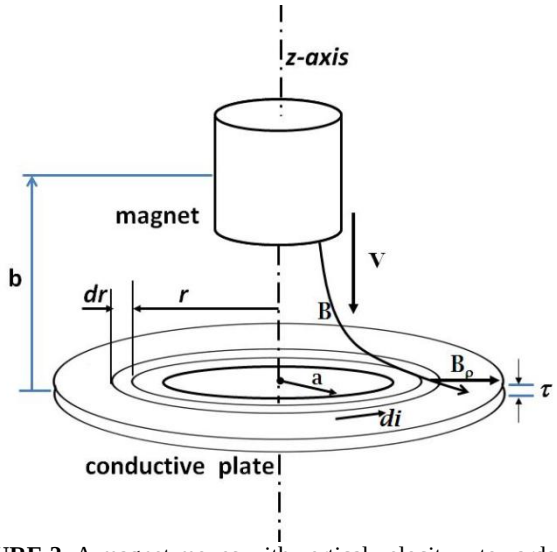

FIGURE 2. A magnet moves with vertical velocity **v** towards the orifice of radius *a* in a conducting plate (of thickness *τ*). A current *di* is induced in an infinitesimal ring element of radius *r* and width *dr*. The magnetic line **B** has a radial component B_ρ at the ring. The magnet-to-orifice separation is *b*.

$$di = \varepsilon_i \frac{(\sigma\tau dr)}{2\pi r} = 2\pi r\, B_\rho(r,b)v\,(\sigma\tau dr/2\pi r)\,, \qquad (2)$$

which is simply the equation of a purely resistive circuit. Note that we are neglecting any inductance effects in the infinitesimal conducting ring considered in Fig. 2, *e.g.* the term *L di/dt* in the circuit equation was neglected. One can easily calculate the inductance *L* of the infinitesimal ring which is of the order of 0.1 μH, therefore any inductance term, or effect depending upon the ratio $\omega L/R$ can be safely neglected in the circuit (as well as any levitating force on the magnet [14] that may be considered). It must also be noted that the so-called *skin depth effect* can be neglected too since in the present case (*~1* Hz oscillations) this depth is of the order of 10 cm, while the thickness of the conducting plates here considered is of the order of a few millimetres [5, 13, 15, 16, 17].

The magnetic interaction force $d\boldsymbol{F} = di\int(d\boldsymbol{l}\times\boldsymbol{B})$ between the magnet and the infinitesimal conducting ring can be found using a well-known relation [11, 12, 13, 18]

$$dF = (di)\,2\pi r\,B_\rho(r,b) = 2\pi r\sigma\tau\,B_\rho^2(r,b)v\,dr\,. \quad (3)$$

Integrating this infinitesimal force from $r=a$ to infinity we get the force between the bored plate and the magnet, *i.e.* the magnet dragging force,

$$F = 2\pi\,\sigma\tau\,v\int_a^\infty B_\rho^2(r,b)r\,dr. \quad (4)$$

Let us now assume, for the sake of simplicity, the *single dipole approximation* to the small magnet. The radial component B_ρ of the field may then be written as (see Appendix A),

$$B_\rho(r,b) = \frac{\mu_0}{4\pi}\frac{3m\,rb}{(r^2+b^2)^{5/2}}\,, \quad (5)$$

where m is the magnetic dipole moment of the magnet. A higher-order approximation, for instance the two-dipole approximation, would indeed be a better one. However, it shall be seen that this time the single dipole approximation proves to be acceptable, as it predicts with good accuracy the results of the experiments performed by us, and described below. Furthermore, it does so without resorting to lengthy and cumbersome mathematical integrals. From Eqs. (4) and (5) we get

$$F = 2\pi\sigma\tau\,v\left(\frac{3m\mu_0}{4\pi}\right)^2\int_a^\infty\frac{(br)^2}{(r^2+b^2)^5}rdr. \quad (6)$$

Let us rewrite the instantaneous vertical magnet-to-hole separation as $b+z(t)$ where $z(t)<<a$ is a small elongation of the magnet oscillation, and b is the initial equilibrium position of the magnet. In our experiments $b<<r$, and we may neglect b^2 with respect to r^2 in the denominator of the integrand in Eq. (6). This integral can then be immediately evaluated, and by further writing $v = \dot{z}\,(t)$ we get

$$F = \frac{3\pi\sigma\tau}{a^4}\left(\frac{m\mu_0}{4\pi}\right)^2\frac{(b+z)^2}{a^2}\dot{z}\,. \quad (7)$$

This is the sought magnetic damping force on the oscillating magnet. It is a viscous force (note its dependence upon the magnet speed $\dot{z}$), but more importantly it is a nonlinear time-varying force since the coefficient of $\dot{z}$ is nonlinear as well as time-varying. It is also a weak force since we are assuming $(b + z(t)) < a$.

When the system in Fig. 1 is set in small amplitude oscillations from a small initial separation $b\sim0$, it is always seen to execute long lasting oscillations of slowly decaying amplitude, and therefore we may rewrite the damping force given in Eq. (7) as

$$F = \frac{3\pi\sigma\tau}{a^4}\left(\frac{m\mu_0}{4\pi}\right)^2\frac{z^2}{a^2}\dot{z} \equiv 2M\lambda_0\left(\frac{z}{a}\right)^2\dot{z}\,, \quad (8)$$

where M is the total mass of the oscillator, and where we have introduced the damping constant λ_0 defined as

$$\lambda_0 \equiv \left(\frac{m\mu_0}{4\pi}\right)^2\frac{3\pi\sigma\tau}{2a^4M}\,. \quad (9)$$

It is important to note that the damping force on the magnet motion is a function of the product $z^2\dot{z}$ (see Eq. (8)), and therefore it becomes zero at the oscillation extremes, and zero once again when the mid-plane of the magnet crosses through the plane of the orifice in the plate. For the latter position, half of the magnet lies over the plate, and the other half below, the radial component B_ρ of the field then being exactly zero at the plate. Therefore we may expect the damping force on the magnet to become practically nil once again for this particular position of the magnet in phase space *(z,v)*.

Having found the expression for the magnetic damping force we can now write the magnet motion equation

$$\ddot{z} + 2\lambda_0\frac{z^2}{a^2}\dot{z} + \omega_0^2 z = 0. \quad (10)$$

In this non-linear equation the constant λ_0 is in fact the damping coefficient for a whole (non-bored) plate. It is interesting to compare Eq. (10) with the motion equation of the usual damped oscillator that contains a viscous term of the form $2\lambda\,\dot{z}$ (λ being a constant), and whose solution is an exponentially decaying function. In the present case we have a non-linear factor proportional to z^2 in the viscous term of the equation.

Equation (10) can be approximately solved in a number of ways, *e.g.* by resorting to numerical integration methods. In this work we shall find particular solutions under some reasonable and sound assumptions *e.g.* assuming *the magnet oscillations to be of small amplitude, and taking into account the truly small damping constant* (in practice $\lambda_0 \ll \omega_0$, see Section IV) *of the system*. With these assumptions in mind, we can find a solution for the motion equation of the oscillator in a simple way using a procedure introduced by Landau and Liftshitz [10], and also used in [3]. It consists in finding an expression that would give us the amplitude A_n of the n-th oscillation cycle in terms of the initial amplitude A_0 of oscillation set by the experimenter. We therefore need to evaluate *the energy lost per oscillation cycle* of the magnet-spring system, which is indeed a small amount of energy due to the actual small damping. To the effect we simply rewrite Eq. (10) as

$$\ddot{z} + \omega_0^2 z = -2\lambda_0\frac{z^2}{a^2}\dot{z}\,. \quad (11)$$

By integrating Eq. (11) along the n-th cycle of oscillation we get the following: from the left hand side of the equation the total energy change *ΔE per unit mass* in the cycle where $E = \left[\frac{1}{2}\dot{z}^2 + \frac{1}{2}\omega_0^2 z\right]_n$, while from the right we get the energy lost due to the damping, again *per unit mass*, during this n-th cycle, *i.e.*

$$\left[\tfrac{1}{2}\dot{z}^2+\tfrac{1}{2}\omega_0^2 z\right]_{n+1}-\left[\tfrac{1}{2}\dot{z}^2+\tfrac{1}{2}\omega_0^2 z\right]_n=\ldots$$
$$-\int_n^{n+1}2\lambda_0\tfrac{z^2}{a^2}\dot{z}\,dz=-\int_{t_n}^{t_{n+1}}2\lambda_0\tfrac{z^2}{a^2}\dot{z}^2dt\ , \qquad (12)$$

which is the essence of the quoted Landau and Lifshitz method.

Eq. (12) is a first order differential equation that can be dealt with by recalling our assumptions that our magnet is oscillating with slowly decaying small amplitudes *A(t)*, whose angular frequency is ω_0, that is we may try a solution of the form

$$z(t)=A(t)\,cos\ \omega_0 t\ . \qquad (13)$$

After replacing this into Eq. (12) and averaging over time along the *n*-th oscillation cycle we get

$$-\Delta E=\langle 2\lambda_0\tfrac{z^2}{a^2}\dot{z}^2\rangle_t\,T_0=$$
$$\int_0^{T_0}\tfrac{\lambda_0}{a^2}\omega_0^2A^4 2\cos^2\omega_0 t\,\sin^2\omega_0 t\,dt, \qquad (14)$$

where T_0 is the period of the oscillations, and $A=A_n$ the amplitude. Therefore

$$-\Delta E=\tfrac{\lambda_0}{2a^2}\omega_0^2\mathrm{A}^4\int_0^{\mathrm{T}_0}\sin^2(2\omega_0\mathrm{t})\ \mathrm{dt}=\tfrac{\lambda_0}{4a^2}A^4\omega_0^2T_0. \qquad (15)$$

Since the total energy *E* of the oscillator may be equated either to its maximum kinetic energy or to its maximum elastic potential energy we may write the simple relation

$$E=\left[\tfrac{1}{2}\dot{z}^2+\tfrac{\omega_0^2}{2}z^2\right]_n=\tfrac{1}{2}\omega_0^2A^2\ , \qquad (16)$$

which also represents the total spring-magnet oscillator energy in the *n*-th oscillation cycle (practically a constant of the oscillations, since the damping is so small), and where $A\equiv A_n= z_n$ is the oscillation amplitude in that cycle. Since both ΔE and T_0 are small we may rewrite the quotient $\Delta E/T_0$ as dE/dt and thence fore

$$\frac{dE}{dt}=-\tfrac{\lambda_0}{4a^2}\omega_0^2A^4. \qquad (17)$$

Furthermore, replacing *E* from Eq. (16) we may write

$$\frac{d\left[\frac{1}{2}\omega_0^{\ 2}A^2\right]}{dt}=-\tfrac{\lambda_0}{4a^2}\omega_0^2A^4\ \Leftrightarrow\frac{dA^2}{(A^2)^2}=-\tfrac{\lambda_0}{2a^2}dt\ . \qquad (18)$$

Integrating (18) between t=0 and $t = nT_0$ with $n \in \mathbb{N}$ (that is between the initial amplitude A_0 and the amplitude A_n of the *n*-th oscillation) we finally get

$$\frac{1}{A_n^2}-\frac{1}{A_0^2}=\tfrac{\lambda_0 T_0}{2a^2}n\ . \qquad (19)$$

This quadratic algebraic equation allows us to obtain the amplitude A_n in any oscillation cycle in terms of the small initial oscillation amplitude A_0 that the experimenter sets at the start of the magnet oscillations.

III. EXPERIMENT SET-UP

As in Fig. (1) a small cylindrical Nd-ferrite magnet (height 3.20 mm, diameter 13.2 mm) of mass 3.20 g was hung from a soft spring of elastic constant 3.31 N/m. Actually the total mass of our oscillating system is 55.4 g (non-magnetic tare was attached to the magnet to increase its inertia and period of oscillation, as well as to ensure smooth oscillations of the system along the vertical). The angular frequency of our freely oscillating magnet-spring system is ω_0 = 7.72 rad/s, a value that corresponds to a natural period of oscillation T_0=0.814 s (accurately measured using a digital scope in previous calibration experiments). The small attenuation constant of the oscillations was measured to range from 0.020 s^{-1} to 0.080 s^{-1} for the different cases presented below. The natural mechanical attenuation of the oscillating system was found instead to be much lower, only 0.003 s^{-1}. A 26.0 mm diameter orifice was bored in a 3.0 mm thick stock aluminium (Alclad 3003-O) plate. The magnet was then set in motion so that it could oscillate symmetrically across this orifice. The electrical conductivity of the aluminium used was previously found (σ =26.9 $Ohm^{-1}m^{-1}$) by measuring the resistance of several long aluminium strips of the material. The magnetic dipole 0.48 Am^2 of the Nd magnet was also found in a previous simple experiment (using a coil instead of the metallic plate, letting the magnet to oscillate inside the coil, and then applying Faraday´s induction law to estimate the dipole [4, 12]).

The vertical position of this oscillating system is reliably monitored using a convenient device already described in previous works [4, 12]. It is a home-made transparent stepped-wedge (about 66 steps) of thin acetate transparency strips carefully stacked so that each step is only about 0.2 mm long. This wedge is attached between the magnet and the spring so that a collimated beam of light from a white-light LED traverses it (Fig. (1)).This stepped wedge exponentially attenuates the beam intensity and the transmitted beam is measured with a photo-transistor followed with a diode connected in series to its emitter. The electrical signal generated is instantaneously displayed in a digital-storage oscilloscope. Previous calibrations show that as this stepped-wedge moves vertically it attenuates the light beam with small error, thus performing as a good linear position transducer for the magnet. The storage oscilloscope not only displays the actual waveform of the magnet oscillations, it also allows to store the waveform in a convenient way for analysis *a posteriori* (no need at all to use image analysis of a video). Not shown in Fig. (1) we attached a 1.5 cm wide acetate strip at the top of the stepped wedge to avoid the magnet to rotate about the vertical. This auxiliary and flexible damper strip, bent as an arch (upward concavity) was fixed between a nearby post and the wedge with a sticker. This stabilizing strip did not add significant friction to the free low frequency oscillation of the system

(the total measured mechanical attenuation constant of the system, flexible strip included is less than 0.003 s^{-1}).

IV. EXPERIMENTS

As explained below we performed two sets of experiments with our system. In the first experiments we initially placed the magnet in coincidence with the orifice *i.e. b=0*. We expected both the damping force on the magnet and the radial field to be small, and then a motion equation with a non-linear damping term proportional to the product $z^2\dot{z}$. For the second set of experiments the magnet was initially placed above the orifice so that *b~a*. Now the attenuation was given by the linear term 2λ(b) *ż*, and as *b* increased the damping coefficient approached the magnetic damping on a magnet that oscillates above a whole conducting plate, as in reference [6].

(A. Small magnet oscillations for separation *b=0*

When *b=0* the magnet mid-plane is coincident with the orifice mid-plane, and the magnet can then be set to oscillate symmetrically with respect to the plate. Fig. 3(a) shows the small amplitude oscillation of the magnet theoretically predicted using the original motion Eq. (10), which we solved using the 4th-order Runge-Kutta method. The plotted envelope of the trace in Fig. 3(a) involves the amplitudes *A(t)* and was obtained instead using Eq. (19) of the Landau-Lifshitz approximation we developed in Section II. Figure 3(a) thus shows the good accuracy obtained by using this approximation: the envelope does match the decaying amplitudes (*i.e.* it involves the oscillations peaks).

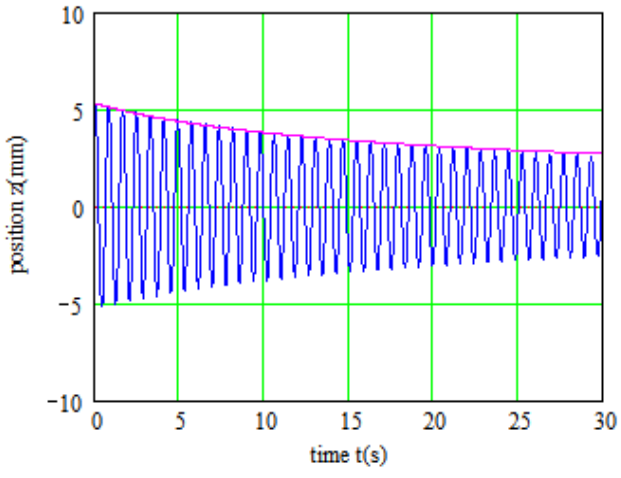

FIGURE 3(a). Predicted oscillations of the magnet: the oscillations obtained numerically solving the motion Eq. (10), for an initial amplitude 5.3 mm. The envelope curve of the oscillations was obtained instead using the quadratic Eq. (21).

Fig. 3(b) shows actual experimental results. It shows the storage-oscilloscope trace of the magnet oscillations recorded for initial amplitude 5.3 mm. Notice the large number of smoothly decaying oscillations recorded in the experiment. The envelope of the oscillations in this figure was again obtained using our Eq. (19), yet this time including the small natural damping of the whole oscillating spring-magnet system (that includes even the friction of the whole system with air (Appendix C)), as well as a correction due to large amplitude oscillations. The agreement between theory and experiment is again very good.

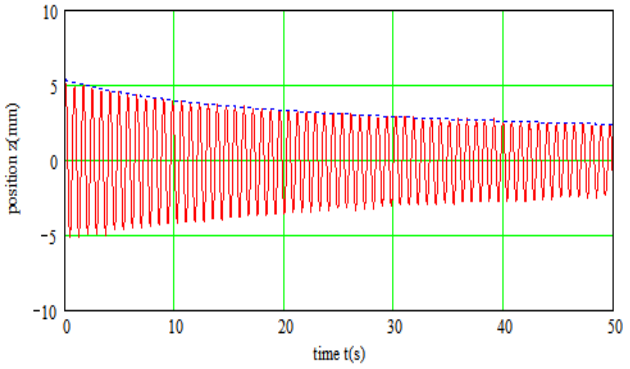

FIGURE 3 (b). Actual experimental oscilloscope trace of the same oscillations and envelope plotted in (a) for an initial amplitude A_0= 5.3 mm (65 smoothly decaying oscillations are shown). This figure is to be compared with Fig. 3(a).

Figure 3(c) shows only a few of the actual oscillations of the magnet in the time interval 10 to 15 s, and with greater detail than in Fig. 3(b). It may be noticed in the figure that the resolution and the linearity of our stepped-wedge-phototransistor detector is good enough not to distort the harmonic nature of the oscillations.

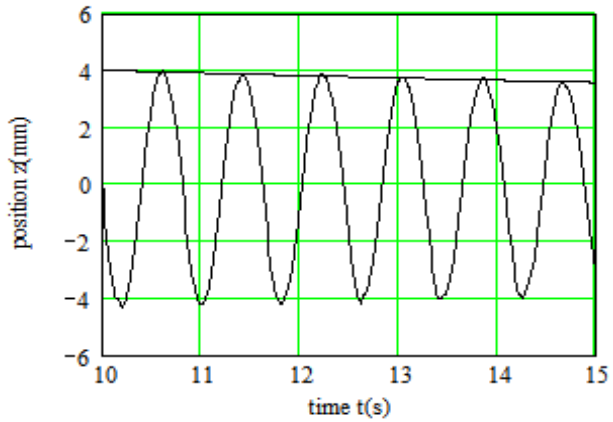

FIGURE 3(c) Details of the oscilloscope trace of the magnet oscillations taken from Fig. 3(b): showing its undistorted quasi-sinusoidal oscillations from 10 to 15 s. This confirms the linearity of our position detection transducer to locate the magnet position as it oscillates.

Figure 4 corresponds to the same experimental data plotted in Fig. 3(b), but instead it shows (lower continuous line) the reciprocal of the squared decaying amplitudes $1/A^2$ as a function of time ($t_n = n\ T_0$) as given by the theory. As a matter of fact Eq. (19) of our analytical model predicts that the experimental data must lie in a straight line. The upper set of plotted points in the figure represents the experimentally measured maxima of the oscillation cycles. The lower set of data points, closer to the continuous line, was obtained by subtracting the natural mechanical damping of the system from the upper set of plotted data points. Again note that the agreement between experimental data and theory is good.

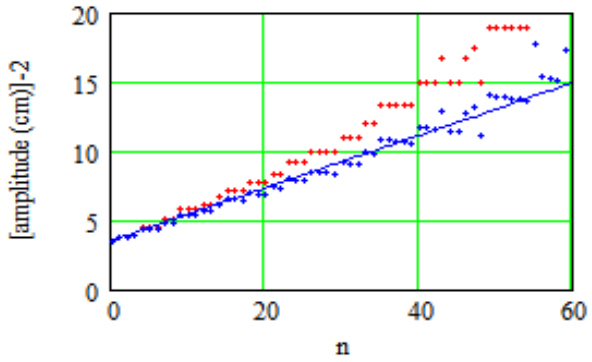

FIGURE 4. Inverse squared amplitudes A_n of the oscillations *vs.* the number n of oscillation cycles (time $t=nT_0$) as obtained from the oscillations in Figure 3(b). The continuous curve is given by Eq. (12). The upper set of points was experimentally obtained with an initial amplitude A_0 = 5.3 *mm*.

B. Small magnet oscillations when $b \neq 0$

We have also studied the case of small oscillations when $b \neq 0$. In this case the integral in Eq. (6) can be evaluated exactly without any approximation (see Appendix B for the case $b \neq 0$). The solution is the damped oscillation expression $z(t) = A_0\ exp[-\lambda(b)t]\cos(\omega_0 t)$ for the magnet position z as given in Appendix B. In these cases we have measured in the laboratory the parameter $\lambda(b)$. In Fig. 5 we have plotted the attenuation constant $\lambda(b)$ of the magnet-spring oscillator for a set of initial equilibrium positions $b \neq 0$ of the magnet with respect to the orifice. The continuous curve in the figure was plotted using Eq. (B4) of the Appendix B. We have also plotted in the figure a dashed curve that bears an interesting relation with the present work: such dashed curve represents the damping coefficient (versus the ratio b/a) when the magnet oscillates above a plate with no orifice in it.

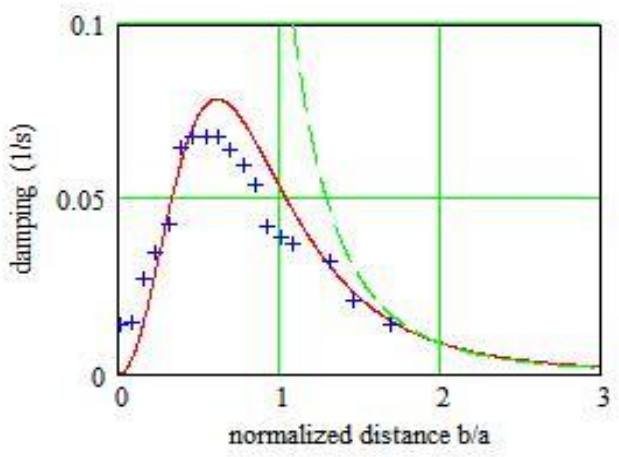

FIGURE 5. Plot of the damping constant of the oscillator versus the separation distance b (equilibrium position of the magnet) in the regime of small amplitude oscillations. The continuous line is given by Eq. (B4) of Appendix B. The dashed line represents the damping on the magnet oscillations over a plate with no orifice.

V. DISCUSSION AND CONCLUSIONS

In this work we have presented a simple mechanical system that consists of a small magnet hung from a vertical spring that executes magnetically damped oscillations across an orifice bored in a metallic plate. The motion equation of the magnet, derived in Section II using basic fundamental principles, happens to be a non-linear differential equation which we approximately solved under two simplifying assumptions: the magnetic drag of the conducting plate on the magnet is weak, and the oscillations of the latter are of slowly decaying amplitudes. Then it was possible to apply an approximate method of solution, based on energy conservation, described in a well-known mechanics textbook [10]. It led us to a much simpler quadratic algebraic equation. Throughout the work we represented the magnet field using the single dipole approximation, which proved to be sufficient to explain satisfactorily our laboratory results. Once the set-up described in Section 3 was ready (with a single piece of equipment, a digital storage oscilloscope), we studied two particular cases of oscillations: (i) when the mean vertical position (equilibrium position) of the magnet oscillations is zero and coincident with the plate mid-plane, *i.e.* $b=0$ in Fig. (1); (ii) when $b \neq 0$. In both cases our theoretical predictions about the motion of the magnet closely matched the experimental results we later obtained in the laboratory. It is interesting to discuss the damping on the magnet motion as a function of the outer radius r_{out} of the bored finite-sized circular plate placed below the magnet. For $a<r_{out}<2a$, *i.e.* outer radius less than about twice the radius a of the orifice, we clearly observed the damping on the magnet motion in its decaying oscillations, and such damping increased with the outer radius of the plate. However, for circular plates of outer radii $r_{out}>2a$ the damping remained practically constant. The reason for this is clear: the Foucault currents

induced by the moving magnet in the bored plate are located, as expected, mostly about the rim of the orifice. By increasing the orifice diameter from *a* to *2a* we lose about 75% of the region of the metallic plate where the Foucault's currents arise. This is concomitant with the $1/a^4$ dependence of the magnetic force obtained in in Eq. (9). Appendices B and C are included to show how our theoretical model and experiments can be extended to study the asymmetrical oscillation, and large amplitude oscillations of the magnet-spring system, respectively (two suitable extensions for a laboratory open-end project). Work is now in progress to solve the non-linear motion equation or our spring-magnet system using numerical methods for both small and large oscillations, and for any value of the parameter *b*. Finally, the oscillating system presented here is a suitable experiment for senior undergraduate physics and engineering students, for an open-end project, as well as for demonstrations. The level of readership is therefore from undergraduate to graduate students, as well as for any university teaching physicist.

ACKNOWLEDGEMENTS

We thank Prof. J. G. Ruiz, Head of Laboratory D, Universidad Simón Bolívar, for providing computer accessories. This work was partially supported by the Decanato de Investigaciones y Desarrollo, Universidad Simón Bolívar (under grant GID-073).

REFERENCES

[1] Kraftmakher Y., *Experiments with a magnetically controlled pendulum*, Eur. J. Phys. **28**, 1007–20 (2007).
[2] Tomasei F. G. and Marconi M. C., *Rolling magnets down a conducting hill: Revisiting a classic demonstration o the effects of eddy currents*, Am. J. Phys. **80**, 800-803 (2012).
[3] Muiznieks A. and Dudareva I., *Quantitative analysis of the damping of magnet oscillations by eddy currents in aluminium foil*, Am J. Phys. **80**, 804-809 (2012).
[4] Ladera, C. L. and Donoso, G., *Anharmonic oscillations of a spring-magnet system inside a magnetic coil*, Eur. J. Phys. **33**, 1259-70 (2012).
[5] Donoso, G. and Ladera, C. L., *Nonlinear dynamics of a magnetically driven Duffing-type spring–magnet oscillator in the static magnetic field of a coil*, Eur. J. Phys. **33** 1473–1486 (2012).
[6] Ladera, C. L. and Donoso, G., *Oscillations of a spring-magnet damped by a conducting plate*, Eur. J. Phys. **34**, 1187-1197 (2013).
[7] Ireson, G. and Twidddle, J., *Magnetic braking revisited: Activities for the undergraduate laboratory*, Eur. J. Phys. **29**, 745-751 (2008).
[8] Donoso, G., Ladera, C. L. and Martin, P., *Damped fall of magnets inside a conducting pipe*, Am. J. Phys. **79**, 193-200 (2011).
[9] Hahn, K D., Johnson, Brokken A. and Baldwin, S., *Eddy current damping of a magnet moving through a pipe*, Am. J. Phys. **66**, 1066-1076 (1998).
[10] Landau, L. D. and Lifshitz, E., *Course of Theoretical Physics Volume 1: Mechanics*, (Pergamon, Oxford UK, 1960), chapter V paragraph 25.
[11] Alonso, M. and Finn, E. J., *Fundamental University Physics II: Field and Waves*, (Addison-Wesley Reading-Massachusetts,1967) chapter 17
[12] Donoso, G., Ladera, C. L. and Martin, P., *Magnetically coupled magnet–spring oscillators*, Eur. J. Phys. **31**, 433-452 (2010).
[13] Griffiths, D. J., *Introduction to Electrodynamics* (Prentice-Hall, Englewood Cliffs, New Jersey, 1981), chapter 8 section 8.3
[14] Tjossem, P. J. H. and Prost, E C, *Optimizing Thomson´s jumping ring*, Am J Phys **79**, 353-358 (2011).
[15] Panofsky, W K H and Philips, M., *Classical Electricity and Magnetism 2*nd edition, (Addison-Wesley, Reading, Massachusetts, 1969), chapter 7.
[16] Davis, L. C. and Reitz, J. R., *Eddy Currents in Finite Conducting Sheets*, J. App. Phys. **42**, 4119-4127 (1971).
[17] Lorrain, P. and Corson, D., *Electromagnetic Fields and Waves*, (Freeman, San Francisco, 1970).
[18] Jackson, J. D., *Classical Electrodynamics*, 3rd Ed., (Wiley, New York, 1999), Chapter 8, section 1.

APPENDIX A

The components of the magnetic field of a magnetic dipole *m* can be written in spherical coordinates (r,θ,φ) as in [18]

$$B_r = \frac{2\mu_0 m}{4\pi}\frac{\cos\vartheta}{r^3}, \qquad B_\vartheta = \frac{2\mu_0 m}{4\pi}\frac{\sin\vartheta}{r^3}. \tag{A1}$$

In cylindrical coordinates (ρ, φ, z), where $\rho=r\sin\theta$ and $z=r\cos\theta$, we have

$$B_z = B_r\cos\vartheta - B_\vartheta\sin\vartheta, \tag{A2}$$

$$B_z = \frac{\mu_0 m}{4\pi}\frac{2\cos^2\vartheta - \sin^2\vartheta}{r^3} = \frac{\mu_0 m}{4\pi}\frac{2z^2-\rho^2}{(\rho^2+z^2)^{5/2}}. \tag{A3}$$

Analogously for the radial component in cylindrical coordinates we get

$$B_\rho = B_r\sin\vartheta + B_\vartheta\cos\vartheta, \tag{A4}$$

$$B_\rho = \frac{3\mu_0 m}{4\pi}\sin\vartheta\cos\vartheta = \frac{\mu_0 m}{4\pi}\frac{3\rho z}{(\rho^2+z^2)^{5/2}}, \tag{A5}$$

which after setting $\rho=r$ it becomes Eq. (5) of the main text.

APPENDIX B. REGIME OF OSCILLATIONS WHEN $b \neq 0$

By making the change $r = bu$ in Eq. (6) of the main text we get

$$F = 2\pi\sigma\tau\, vb^2 \left(\frac{3m\mu_0}{4\pi b^3}\right)^2 \int_{\frac{a}{b}}^{\infty} \frac{u^3}{(1+u^2)^5}\, du, \qquad \text{(B1)}$$

This leads us to evaluate the following indefinite integral

$$\int \frac{u^3}{(1+u^2)^5}\, du = \frac{-(1+4u^2)}{24(1+4u^2)^4} + constant, \qquad \text{(B2)}$$

and to introduce the result in (B1); by further changing back to the variable r, the magnetic interaction force between plate and magnet can then be written as

$$F = \left(\frac{m\mu_0}{4\pi}\right)^2 \frac{3\pi\sigma\tau}{2a^4} \frac{b^2}{a^2} \frac{a^6(b^2+4a^2)}{4(b^2+a^2)^4} v\,. \qquad \text{(B3)}$$

Introducing now the constant λ_0 defined in Eq. (9) of the main text, and the new attenuation coefficient $\lambda(b) = \frac{F}{2Mv}$ we get

$$\lambda(b) = \lambda_0 \left(\frac{b^2}{a^2}\right) \frac{a^6(b^2+4a^2)}{4(b^2+a^2)^4}\,. \qquad \text{(B4)}$$

And thus we arrive to the new motion equation of the oscillating magnet for cases when $b \neq 0$, *i.e.* when the magnet is initially separated from the orifice,

$$\ddot{z} + 2\lambda(b)\, \dot{z} + \omega_0^2 z = 0\,. \qquad \text{(B5)}$$

Note that when $b = z(t) << a$ the second fraction in Eq. (B4) becomes unity, and then we recover our motion Eq. (10) of the main text, as expected. But, when $b \neq 0$ and when the oscillations are of small amplitude the motion equation is linear in z and accept the well-known solution $z(t) = A_0\, exp[-\lambda(b)t]\, \cos(\omega_0 t)$, as already considered in the second set of experiment (see Section IV-b).

APPENDIX C. LARGE AMPLITUDE OSCILLATION REGIME

When the oscillation are of large amplitude, and about $z=0$ the energy lost per cycle as given by Eq. (14) must be corrected by introducing a damping $\lambda(b)$, instead of λ_0, in that equation, and also realizing that now $b=z(t)$, therefore the energy lost ΔE becomes

$$\Delta E = -\int_{t_n}^{t_{n+1}} 2\lambda(z) \frac{z^2}{a^2} \dot{z}^2 dt\,, \qquad \text{(C1)}$$

where now $\lambda(z)$ is given by $\lambda_0 f(z)$, with the function $f(z)$

$$f(z) = \frac{a^6(z^2+4a^2)}{4(z^2+a^2)^4} = \frac{1+\frac{u^2}{4}}{(1+u^2)^4}\,, \qquad \text{(C2)}$$

where for convenience we have just set $u=z/a$. By expanding the denominator on the right hand side of this equation as a binomial we get

$$f(u) \approx \left(1+\frac{u^2}{4}\right)(1-4u^2+6u^2+\cdots) = 1-\frac{15}{4}u^2 + 5u^4 + \cdots.$$

The integral in Eq. (C2) can now be re-written with $b=z$ and then we get

$$\Delta E \approx \int_0^T 2\lambda_0 \frac{z^2}{a^2}\left[1-\frac{15}{4}\left(\frac{z}{a}\right)^2 + 5\left(\frac{z}{a}\right)^4\right] \dot{z}^2 dt\,. \qquad \text{(C3)}$$

It should be noticed that the integral of the first term in the square bracket of this equation recovers the ΔE already considered in the main text (Section II, Eq. (16)) as it should be. However, note that now two additional energy terms have appeared in Eq. (C3). By averaging over an oscillation cycle, as already done in the main text, we get

$$\mathrm{E} = \left[\frac{1}{2}\dot{z}^2 + \frac{\omega_0^2}{2}\mathrm{z}^2\right]_{\mathrm{n}} = \frac{1}{2}\omega_0^2 \mathrm{A}^2 \left[1-\frac{15}{8}\left(\frac{\mathrm{A}}{\mathrm{a}}\right)^2 + \frac{15}{8}\left(\frac{\mathrm{A}}{\mathrm{a}}\right)^4\right]. \qquad \text{(C4)}$$

This equation allows us to write the new damping coefficient for the case of large amplitude oscillations, which is given (as a function of A/a) by

$$\lambda\left(\frac{A}{a}\right) = \lambda_0\left[1-\frac{15}{8}\left(\frac{A}{a}\right)^2 + \frac{15}{8}\left(\frac{A}{a}\right)^4\right]. \qquad \text{(C5)}$$

And now Eq. (19) of the main text must be rewritten, for large-amplitude oscillations, to read,

$$\frac{1}{A_n^2} - \frac{1}{A_0^2} = \frac{\lambda_0}{2a^2}\left[1-\frac{15}{8}\left(\frac{A}{a}\right)^2 + \frac{15}{8}\left(\frac{A}{a}\right)^4\right] nT_0\,. \qquad \text{(C6)}$$

For the particular case when A/a = 5.3/13.0 the second term in the square bracket of this equation represents a correction of 0.312.

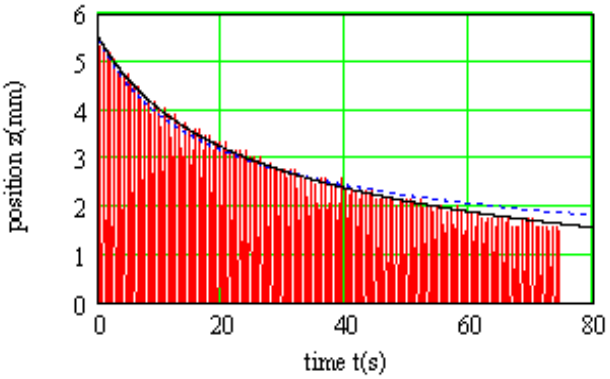

FIGURE C1. Actual half-oscillations of large amplitude for b=0. Two lines have been drawn to envelope the amplitudes of oscillation: the dotted line was drawn using Eq. (19), while the solid envelope was obtained with Eq.(C6), that includes the correction for the amplitudes of oscillation being large.

Figure C1 shows actual experimental half-oscillations of large amplitude (oscilloscope traces) involved with envelopes given by Eq. (12), the dotted line, as well as with Eq. (C6), the solid line, respectively. It may be seen that the dotted envelope (obtained for small-amplitude oscillations) departs from the experimental results as time goes by, while the continuous envelope obtained using the large-amplitude oscillations model, just derived in this Appendix, do involve the peaks of the oscillations, as it should be.